Study of Divergence in the Boundary Layer Using Optical Propagation Techniques[1]

A. G. KJELAAS

Norwegian Defence Research Establishment, Kjeller

G. R. OCHS

Environmental Research Laboratories, NOAA, Boulder, Colo. 80302

(Manuscript received 25 July 1973, in revised form 27 November 1973)

ABSTRACT

A wind-measuring system using three separate optical systems, each consisting of a 3 mW He-Ne laser and two photodiode receivers, forming an equilateral triangle 300 m on a side, has successfully measured the divergence over the area of the triangle, and the space-averaged horizontal wind vector. Good correlation was found between the flow into the triangle and occurrences of thermal plumes seen by an adjacent acoustic sounder. The flow into the triangle was proportional to the vertical velocity. During large convective activity, there was a certain periodicity in the occurrence of plumes.

1. Introduction

Reliable measurements of the divergence of the horizontal wind are difficult to achieve. Many attempts have been made to develop methods based on point measurements of wind. On the synoptic scales, Bellamy (1949) developed a technique that used a triangle of wind reports to calculate the divergence for the enclosed area; Endlich and Clark (1963) calculated divergence by linear interpolation between wind components at the vertices of the triangle of observation. Eddy (1964) improved Bellamy's triangle technique by using a computer model. He also applied a correlation technique to establish the space correlation and time persistence.

On smaller scales (i.e., those scales comparable with plumes and on up to a few hundred meters), no reliable techniques for measuring the horizontal divergence exist. Many laboratory experiments have formed the basis for different theories for entrainment into plumes. Morton *et al.* (1956) have described a model assuming that the rate of entrainment into the plumes is proportional to the vertical velocity inside the plume. Telford (1966) has developed a model assuming that the entrainment should not be related to the mean velocity but to the local level of turbulence.

Due to lack of suitable wind-measuring techniques these theories have been difficult to check in the atmosphere. Recently, remote sensing of space-averaged wind has progressed, making it possible to calculate the divergence for a small enclosed area. Lawrence *et al.* (1972) have described an optical wind sensor that uses the naturally occurring density fluctuations to obtain a spatially averaged wind. By using a correlation technique at the receiver, they are able to extract a path-averaged transverse wind speed.

This paper discusses field measurements of divergence and wind velocity based on an extension of the optical technique. A He-Ne laser triangle path (300 m on a side) was set up near a 150 m tower. The results are compared with wind velocity measured at five levels on the tower and with the occurrence of plumes as seen by an acoustic sounder located inside the triangle.

2. The optical measuring equipment

The optical technique used for wind measurement is described fully in Lawrence *et al.* (1972); however, a brief discussion is included here for completeness, since it is a recent development. The technique may be used over ranges from 300 m to more than 15 km, so that it is particularly useful for obtaining spatially averaged wind measurements. In addition, it is effective for measuring low mean wind flow in the presence of large fluctuating components.

The technique uses the drifting scintillation pattern arising from wind-transported refractive-index irregularities in the atmosphere. This drifting scintillation pattern is the cause of the twinkling, or scintillation, of starlight. With a very small, bright light source, such as a laser shining through the atmosphere, the moving scintillation pattern can be seen clearly on a screen at night. The sizes of the irregular patches of light in the pattern are determined by the diffraction of the incident beam; they result from refractive-index irregularities

[1] The paper was prepared while the senior author was a visiting scientist at the National Oceanic and Atmospheric Administration, Environmental Research Laboratories, Boulder, under sponsorship of the Royal Norwegian Council for Scientific and Industrial Research.

(almost entirely the result of temperature differences) at various positions along the propagation path. At each position, the diffraction process selects a most effective scale of irregularity, or eddy, whose size is sufficient to cause a half-wavelength difference in path-length to the receiver for two extreme rays passing through its edges. The diffraction effects of this particular eddy dominate over those of other eddies at the same location.

If a diverging laser beam is effectively a point source, geometric magnification increases the size of the received eddy image by the factor L/z, where z is the position along a beam of length L. The image drift rate at the receiver caused by the local eddy drift velocity, depending on the wind at position z, is also increased by the same factor. Therefore, the received optical disturbance is larger and moves faster than the eddy that produced it. Since different portions of the path contribute to the total scintillation pattern, that pattern will be continuously evolving because of the relative speeds of the different sized features it contains.

To measure the average component of the wind across an optical path, we look at fluctuations in light intensity in two small apertures spaced along the direction of movement of the pattern, as shown in Fig. 1. A function like that shown in Fig. 2 results if the normalized covariance of the logarithms of these signals is computed. For the conditions of a uniform wind at right angles to the optical path and parallel to the separation of the detectors, and for uniform refractive-index structure constant (C_n^2) along the path, some measure of the time scale of the function, e.g., the time delay to the peak or the slope of the function at zero delay, could be used to derive wind speed. For the real case, with winds of arbitrary direction and speed along the path, and with a non-uniform distribution of C_n^2 along the path, this function changes not only in time scale, but also in shape. It can be shown (Lawrence *et al.*, 1972), for uniform C_n^2 along the path, that the slope of the function at zero delay has a known relationship to the average horizontal wind across the path, even though the wind along the path is non-uniform in direction and speed. Thus, we measure the slope at zero delay to determine the average wind. The weighting function of the wind measurement for various receiver separations is shown in Fig. 3 as a function of $\beta=\rho(\lambda L)^{-\frac{1}{2}}$, where ρ is the detector spacing, λ the laser wavelength, and L the path length. For the divergence

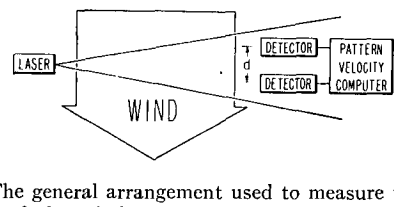

FIG. 1. The general arrangement used to measure the average component of the wind, across a laser beam, parallel to the (usually horizontal) spacing of two detectors.

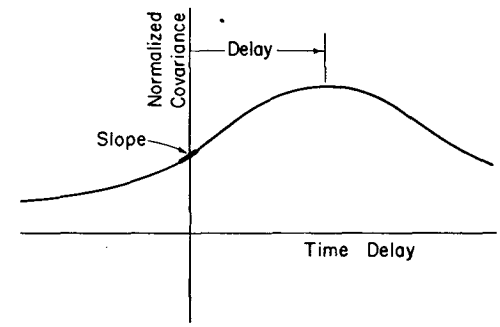

FIG. 2. A schematic diagram of the normalized covariance function, showing the delay to the peak and the slope at zero time lag. While the former is frequently used to measure pattern drift velocities, the latter is more suitable in the optical case where the pattern decays rapidly.

measurement reported here, $\beta=0.46$. This separation, and the use of apertures 6 mm in diameter, gave a nearly symmetrical weighting function around the center of the path.

There are several limitations to the present optical system, but we no not believe that they affected the wind measurements reported here. The wind weighting function is strictly correct only when the wind measurement is averaged over enough time so that C_n^2 is statistically uniform over the path. This can be satisfied for a horizontal path, but if, for example, a slant path is used C_n^2 will tend to be higher at the lower end of the path, and the wind in this portion will be weighted more heavily. Random variations of C_n^2 will distort the measured average wind speed only if they are correlated with the variations in wind speed. A reasonable supposition is that turbulence is strongest at locations of maximum wind shear, not at locations of maximum wind speed. If so, the turbulence tends to be uncorrelated with the wind, and the average obtained by the

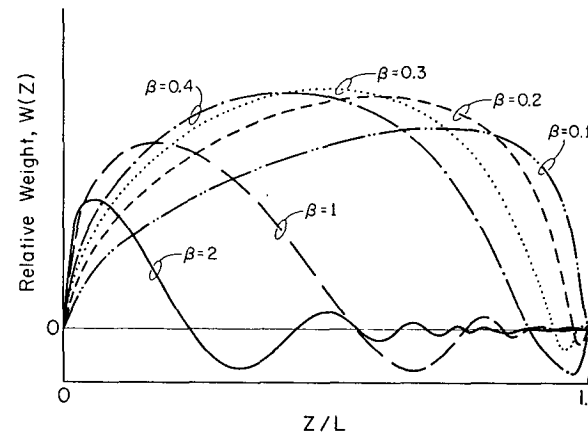

FIG. 3. The relative weights of the different portions of the path in determining the optically measured wind. The parameter $\beta=\rho(\lambda L)^{-\frac{1}{2}}$ is the separation of the sensors. These curves are calculated for point sensors; the finite area of a real sensor will tend to remove the negative weights near the receiver.

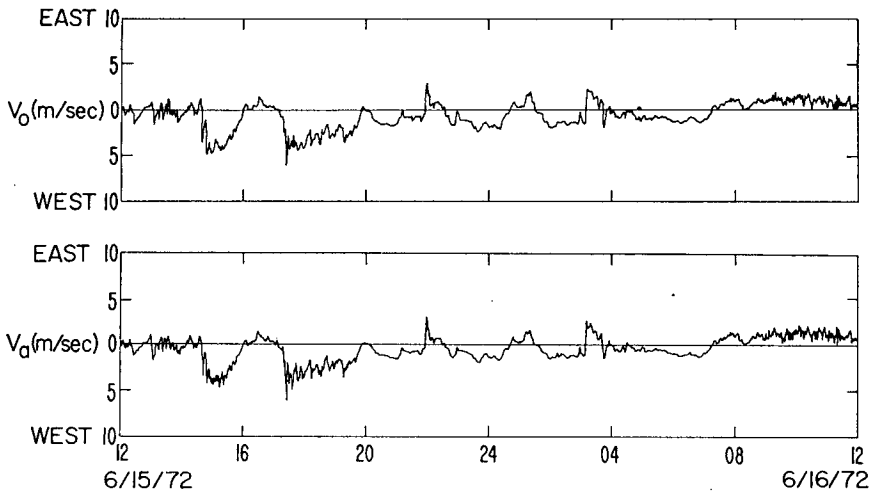

FIG. 4. A comparison of the average wind speed (V_0) measured optically, with the average of the readings of six Gill propellor anemometers (V_a) uniformly spaced along the optical path. Both the anemometers and the optical system measure the component of wind that is horizontal and at right angles to the path. The path is 300 m long, oriented north–south, and 3 m above the ground.

optical system is unbiased. A second source of error may occur when there is a combination of high refractive-index fluctuations and long path. Under these conditions, a so-called saturation effect occurs, in which the optical scintillation no longer increases with C_n^2. When this condition occurs, the spherical propagation equations upon which the optical wind measurement is based are no longer correct. The result is that the optical measurement will underestimate the true wind, and in severe saturation this may be by a factor of 2 or more. Saturation may be easily detected by the optical system and did not occur on the 300 m paths used in our divergence experiment.

Before undertaking the divergence experiment, we compared the average wind speed reading of one of the three optical systems, over the same height and path length that was later used, with the average of the readings of six Gill propellor anemometers uniformly spaced along the optical path. The anemometers were oriented to read the component of wind that was horizontal and at right angles to the optical path. The result for a 24-hr period is shown in Fig. 4 and appears to offer full proof of satisfactory performance.

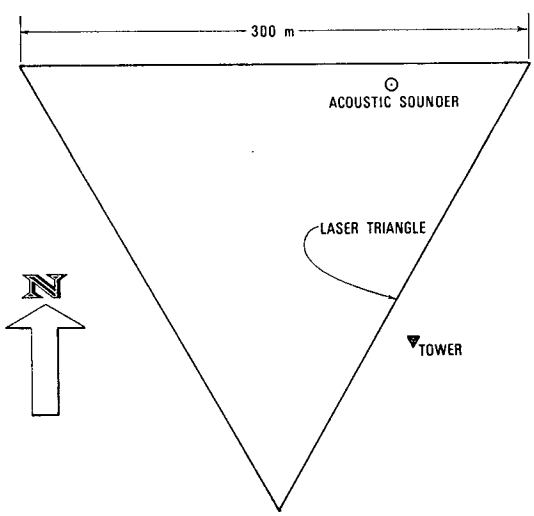

FIG. 5. The layout of the laser triangle, 150 m meteorological tower, and the acoustic sounder.

3. Measurement and data reduction

The measurements were made at Haswell, Colo., during a two-week period in the beginning of August 1972. The Haswell area has a typical high-plain meteorological regime with strong radiative cooling during the night and strong solar heating and convective activity during the day.

Three separate optical systems, each consisting of a 3-mW He-Ne laser, two photodiode receivers, and a small specialized computer providing a real-time read-out of average wind speed, were used in the experiment. The optical paths formed an equilateral triangle, 300 m on a side and 2.3 m above the ground. Fig. 5 shows the location of the laser triangle relative to the meteorological tower and the acoustic sounder. The terrain near the triangle is flat and free from any obstacles for a minimum of 3 km in any direction. The area is covered with clumps of buffalo grass (~15 cm in height). Since each optical path was arranged to read an outflowing wind as positive, the sum of the readings of all three paths represents the average horizontal wind speed out of the triangle. The individual wind readings for each optical path, smoothed with a 10-sec running average, as well as the scalar sum of all three, were recorded

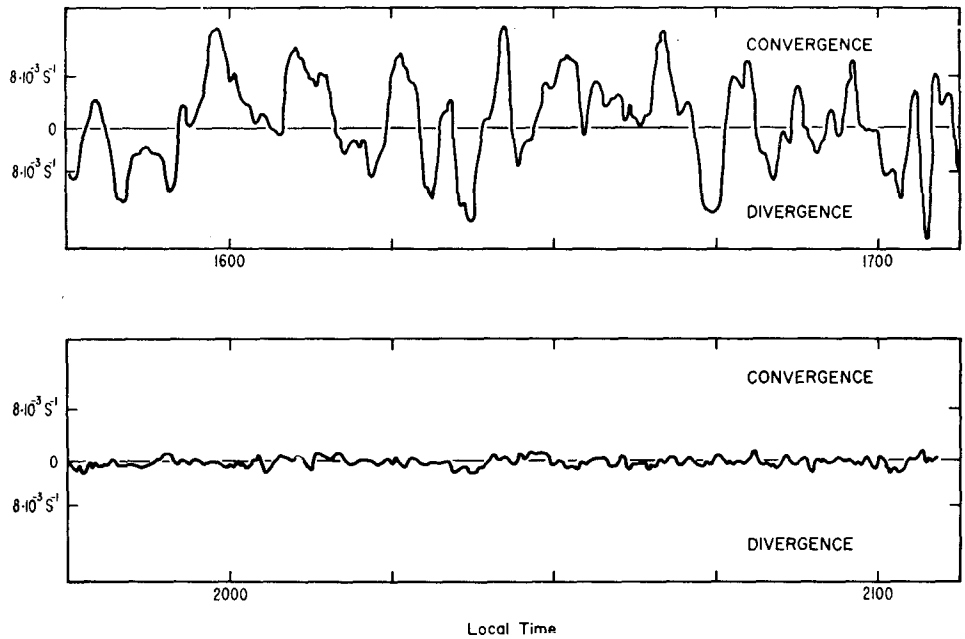

FIG. 6. Ten-second average divergence recordings for typical afternoon and night periods.

simultaneously on strip chart recorders and on a digital tape recorder.

The horizontal wind divergence is given by

$$\nabla_h \cdot \mathbf{V} = \frac{L(v_0 + v_{120} + v_{240})}{A},$$

where v_0, v_{120}, v_{240} are the wind components transverse to the east-west, 30°-210° and 150°–330° triangle sides, respectively; L is the side of the triangle; and A the area of the triangle.

Typical recordings of divergence during periods of large convective activity and stable conditions are shown in Fig. 6. Convergence of 10^{-2} sec^{-1} over periods of minutes is common during daytime. During the night, values of 5×10^{-4} sec^{-1} are normal. This value may be considered the upper limit of the noise level of the divergence measurement. In the comparison between divergence and vertical velocity, a 100-sec running average was used. The space-time average wind velocity was computed by using the wind components measured over two of the triangle sides. This, of course, gives a redundant estimate of the velocity as we have three pairs of legs on a triangle.

Using, for example, the east–west and 30°–210° pair, the horizontal space average wind speed $\bar{V}_s$ can be expressed in terms of the two components v_0 and v_{120} as

$$\bar{V}_s = \left[\left(\frac{2v_{120}+v_0}{3}\right)^2 + v_0^2\right]^{\frac{1}{2}},$$

and the direction α from which the wind is blowing as

$$\alpha = \tan^{-1}\left(\frac{v_0\sqrt{3}}{2V_{120}+v_0}\right)+180°.$$

Using the other pairs of the triangle, similar expressions are obtained.

The meteorological tower was instrumented to measure vector wind by the use of bivanes at five fixed levels: 31, 62, 93, 124 and 149 m. The acoustic sounder inside the triangle was pointing vertically, and its records were compared with the measured inflow into the triangle. All data, except the acoustic sounder data, were sampled once per second and recorded on digital tapes. The acoustic sounder data were recorded (both) on facsimile and analog tapes.

4. Results

a. Comparison of divergence and the acoustic sounder

Considerable evidence now exists that plume-like structure can be seen by an acoustic sounder (McAllister *et al.*, 1969; Beran, 1971). Fig. 7 shows an acoustic sounder record and a divergence for predominately large convective activity. The dark portions on the sounder record correspond to thermal plumes and their height indicates the height of the plumes, while the white "gaps" are interpreted as area between plumes. The solid line is the divergence measured by the optical system. Convergence is upward on the figure.

The correspondence between the measured convergence and the plumes as seen by the acoustic sounder is mostly good, although some discrepancies can be seen especially after 1440 local time. Note that while the divergence is measured at a height of about 2 m above ground, the lowest height seen by the acoustic sounder is about 50 m, making an absolute comparison between the two systems difficult.

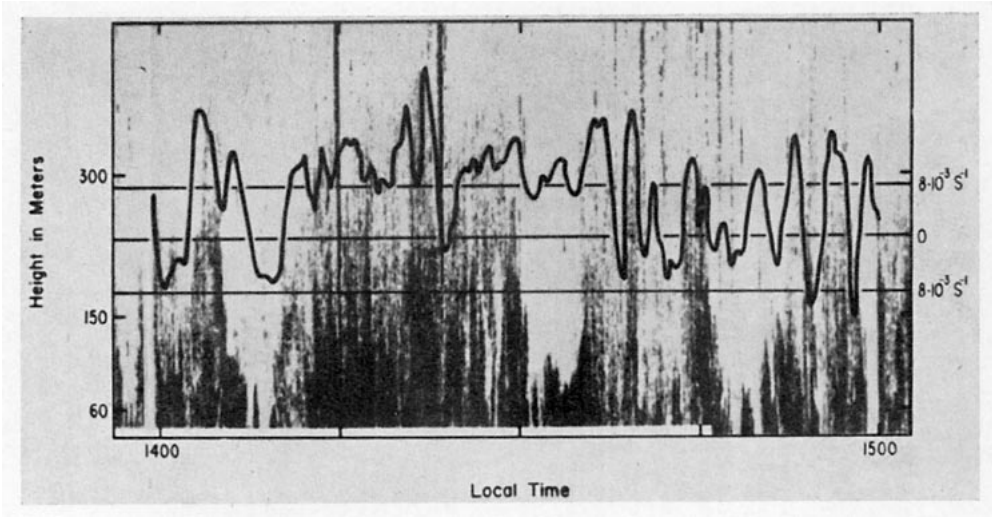

FIG. 7. Comparison between the plumes seen by the acoustic sounder and the flow into the triangle. Large plumes are associated with large convergence. The solid line is the divergence measured by the optical system.

b. Correlation of divergence and vertical wind

The vertical velocity is related to the divergence field through the equation of continuity as

$$\nabla_h \cdot \mathbf{V} = -\frac{\partial w}{\partial z}.$$

Fig. 8 shows a typical set of cross-correlation curves between the divergence and the vertical wind and gradient on the tower during strong convective activity.

Because the tower is outside the triangle, the peak in the cross correlations does not occur at zero lag but is shifted in time corresponding to the travel time between the tower and the center of the triangle. For the case chosen the wind direction was along a line between the center of the triangle and the tower. The negative lag means that the divergence is lagged behind the vertical wind on the tower.

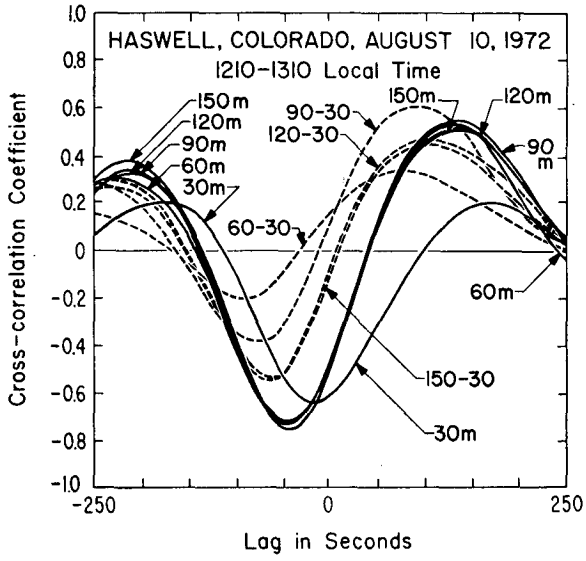

FIG. 8. Cross-correlation curves between divergence and vertical wind, and divergence and vertical wind gradient for the different levels on the tower. Solid lines are divergence vs vertical velocity and dotted lines divergence vs vertical wind gradient.

One of the interesting features in Fig. 8 is the difference in correlation between $\nabla_h \cdot \mathbf{V}$ and $-\partial w/\partial z$, and between $\nabla_h \cdot \mathbf{V}$ and w. From these curves, we see that in the case of plumes, the convergence into the plumes is more determined by the vertical wind than by the gradient of the same. These results seem to agree with Morton *et al.* (1956), who assumed that the entrainment into plumes was proportional to the upward velocity. It might be argued that this picture might have been different if we had had a measurement of the vertical wind at the same height as the divergence measurement. Due to the 100-sec running average, however, we are looking at a large population of plumes which should not differ much from 5 to 30 m, so we believe that our results give a reasonably correct picture.

Another interesting feature of these curves is the relative time shift between the peaks in the cross correlations for the vertical wind at the different levels indicating that the plumes or convective currents are tilted. The tilt is in the downwind direction. This corresponds to what Kaimal and Businger (1970) have reported for a single plume. The plumes are passing the four upper levels on the tower at about the same time but some 20–30 sec earlier than the lowest level (30 m).

In all the cases we have analyzed, the plumes were tilted in the lowest 60 m, whereas from 60 to 150 m almost no tilting was observed.

The third feature that should be observed in Fig. 8 is the periodicity in the cross-correlation curves indicating that there is a periodicity in the development of con-

vective currents in the boundary layer. The time between the two cross-correlation maxima, which might be interpreted as the period between a set of plumes, is 360 sec.

Panofsky (1973) has recently shown that the plumes seem to move with a speed close to the local wind. In this case the wind was about 1.5 m sec^{-1} at the height of the triangle, giving us a separation in space of about 540 m between every major set of plumes. This scale size seems to agree with what Ackerman (1967) has reported for convective clouds. She found scale sizes of 400–900 m. This periodicity was only found during large convective activity. During the morning and the evening hours correlation curves like curve B shown in Fig. 9 are typical. The magnitude of the correlation between $\nabla_h \cdot \mathbf{V}$ and w seems to change very little during the day, but the plumes are released more randomly with no outstanding size contributing to the cross correlation during the morning and evening hours.

c. Daily variation of the divergence

As shown in Fig. 6, a great difference exists between the divergence during day and night. In the morning and evening, we found that the flow was out of the triangle about 60% of the time. During heavier convective activity in the middle of the day, the flow was into the triangle 60% of the time. In the middle of the day peak values in convergence (10^{-2} sec^{-1}) were found over periods of 1–2 min. The standard deviation was normally in the order of 4×10^{-3} sec^{-1}.

d. Space average of wind velocity

As shown in Fig. 4, this technique measures the transverse space-averaged wind component. By combining two components as shown in Eqs. (2) and (3), we get the total horizontal wind vector. Since three components are available, these can be combined to give three values of the wind vector. By applying a 20-min running average to the data to smooth out convective activity and comparing these three values, we have a measure of the ability of the system to obtain the space-time averaged horizontal wind vector.

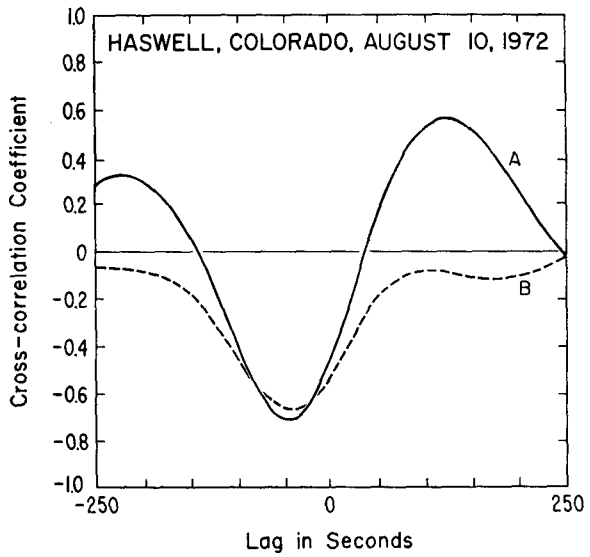

FIG. 9. Cross-correlation curves between divergence and vertical wind. The solid line is for high convective activity, and the dotted line for low convective activity.

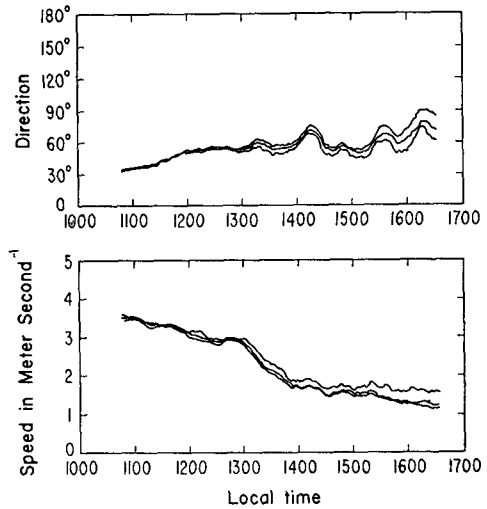

FIG. 10. A comparison of the three values of the wind vector determined from the laser triangle. Wind direction and speed are shown in the upper and lower parts of the figure, respectively. A 20-min running average has been applied to the data to smooth out the effect of convective activity.

Fig. 10 shows plots of the three values of the wind vector for nearly 6 hr, with direction and speed shown in the upper and lower parts of the figure, respectively. For a wind speed higher than about 2 m sec^{-1}, we see that it makes little difference which two of the three components are used to calculate the horizontal wind vector. When the wind speed drops below about 2 m sec^{-1} the differences increase, very likely from several causes. Due to slight differences in the terrain along the triangle legs, irregular wind patterns can persist over the triangle and be more pronounced during light wind conditions. In addition, instrumental errors appear as a fraction of the full-scale wind setting chosen, which was 10 m sec^{-1} for the case shown. Recent modifications to the instrumentation have reduced this source of error.

Figs. 11 and 12 compare the wind speed and direction calculated from the component measurement and the same quantities measured at the 30-m level on the tower. All recordings are 10-sec averages. The wind recordings at the tower are shifted 40 sec in time to compensate for the travel time from the triangle to the tower. The differences in the wind speed magnitude are expected because of the difference in height above ground. Using the logarithmic wind profile to calculate the wind speed at the 30 m level from the wind speed measured with the optical technique, we obtain the

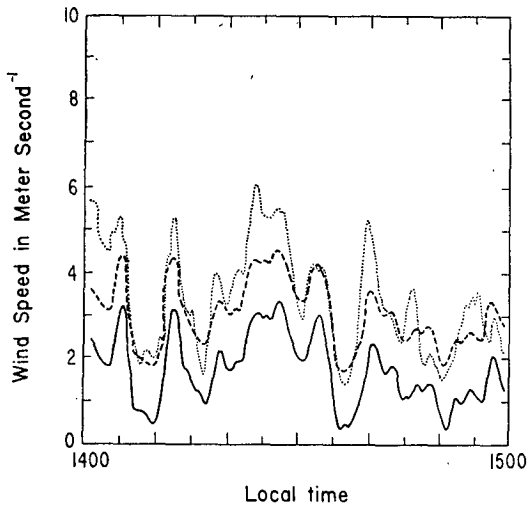

FIG. 11. Comparison of wind speed measured at the 30 m level on the tower (dotted line) with the wind speed calculated from the triangle measurement (solid line). The dashed line is the calculated logarithmic wind profile using a roughness parameter z_0 of 4 cm, and a friction velocity u_* of 20 cm sec^{-1}.

dashed line curve shown in Fig. 11. A roughness parameter z_0 and a friction velocity u_* of 4 cm and 20 cm sec^{-1}, respectively, were used. These values are regarded as reasonable for the type of ground cover and wind speed we encountered.

The correlation between the two types of measurements is very good. The larger variance of the wind measured at the tower is expected because this is a point measurement, while the optical wind measurement is an average both in time and space.

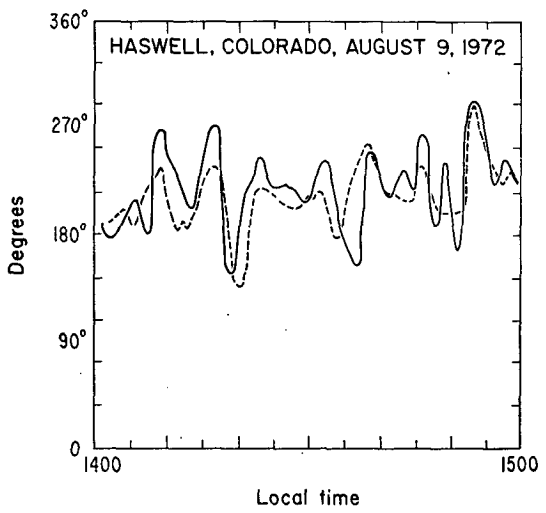

FIG. 12. Comparison of wind direction measured at the 30 m level on the tower (dotted line) and that calculated from the laser wind measurement (solid line).

5. Conclusion

It has been shown that a wind measuring system using three separate optical systems, each consisting of a 3 mW He-Ne laser and two photodiode receivers, forming a equilateral triangle, is successful in measuring the divergence over a small enclosed area. By using two of the optical systems, we can get a space-averaged horizontal wind vector. The thermal plumes as seen by the acoustic sounder and the convergence compare well. The correlation between the divergence and the vertical wind measured on the tower shows that the entrainment into plumes is proportional to the vertical velocity.

During periods with large convective activity a certain periodicity in the development of plumes is found.

Acknowledgments. The senior author expresses his sincere gratitude to Dr. C. Gordon Little, Director of the Wave Propagation Laboratory, for providing him with the opportunity and making the facilities available to make this study while on leave from the Norwegian Defence Research Establishment. The authors also thank Mr. R. S. Lawrence, who initiated this study. Finally, the senior author wants to thank the many members of the Wave Propagation Laboratory who not only contributed with helpful discussions and suggestions, but also created a stimulating environment and accepted him as one of their own.

REFERENCES

Ackerman, Bernice, 1967: The nature of the meteorological fluctuations in clouds. *J. Appl. Meteor.*, **6**, 61–71.

Bellamy, J. C., 1949: Objective calculations of divergence, vertical velocity and vorticity. *Bull. Amer. Meteor. Soc.*, **30**, 45–49.

Beran, D. W., 1971: Acoustics: a new approach for monitoring the environment near airports. *J. Aircraft*, **8**, 934–936.

Eddy, A. 1964: The objective analysis of horizontal wind divergence fields. *Quart. J. Roy. Meteor. Soc.*, **90**, 424–440.

Endlich, R. M., and J. R. Clark, 1963: Objective computations of some meteorological quantities. *J. Appl. Meteor.*, **2**, 66–81.

Kaimal, J. C., and J. A. Businger, 1970: Case studies of a convective plume and a dust devil. *J. Appl. Meteor.*, **9**, 612–620.

Lawrence, R. S., G. R. Ochs and S. F. Clifford, 1972: The use of scintillations to measure average wind across a light beam. *Appl. Opt.*, **11**, 239–243.

McAllister, L. G., J. P. Pollard, A. R. Mahoney and P. J. R: Shaw, 1969: Acoustic sounding—a new approach to the study of the atmospheric structure. *Proc. IEEE*, **57**, 579–587.

Morton, B. R., G. I. Taylor and J. W. Turner, 1956: Turbulent gravitational convection from maintained and instantaneous sources. *Proc. Roy. Soc., London*, **A234**, 1-23.

Panofsky, H. A., 1973: Structure of turbulence. *IFYGL Bull.*, No. 7, 48–49.

Telford, J. W., 1966: The convective mechanisms in clear air *J. Atmos. Sci.*, **23**, 652–666.